

Direct Observation of a Localized Magnetic Soliton in a Spin-Transfer Nanocontact

D. Backes,^{1,*} F. Macià,^{1,2} S. Bonetti,^{3,4} R. Kukreja,^{3,5} H. Ohldag,^{1,6} and A. D. Kent¹

¹*Department of Physics, New York University, 4 Washington Place, New York, New York 10003, USA*

²*Grup de Magnetisme, Departament de Física Fonamental, Universitat de Barcelona, Barcelona 08028, Spain*

³*Stanford Institute for Materials and Energy Sciences, SLAC National Accelerator Laboratory, 2575 Sandhill Road, Menlo Park, California 94025, USA*

⁴*Department of Physics, Stanford University, Stanford, California 94305, USA*

⁵*Department of Materials Science and Engineering, Stanford University, Stanford, California 94305, USA*

⁶*Stanford Synchrotron Radiation Laboratory, 2575 Sandhill Road, Menlo Park, California 94025, USA*

(Received 3 April 2015; published 17 September 2015)

We report the direct observation of a localized magnetic soliton in a spin-transfer nanocontact using scanning transmission x-ray microscopy. Experiments are conducted on a lithographically defined 150 nm diameter nanocontact to an ultrathin ferromagnetic multilayer with perpendicular magnetic anisotropy. Element-resolved x-ray magnetic circular dichroism images show an abrupt onset of a magnetic soliton excitation localized beneath the nanocontact at a threshold current. However, the amplitude of the excitation $\approx 25^\circ$ at the contact center is far less than that predicted ($\lesssim 180^\circ$), showing that the spin dynamics is not described by existing models.

DOI: 10.1103/PhysRevLett.115.127205

PACS numbers: 75.25.-j, 75.30.Ds, 85.75.-d

Spin-torque nano-oscillators (STNOs) are nanometer-scale contacts to thin magnetic layers that enable the generation of high current densities of spin-polarized electrons. Injection of spin-polarized electrons into a ferromagnet leads to dynamic excitations of the magnetization associated with the generation of spin waves. Electrical studies of STNOs have, indeed, revealed such excitations at GHz frequencies [1,2]. In addition, an upper limit to the spatial extent of the spin excitation in layers with in-plane magnetic anisotropy has been measured in Brillouin light scattering experiments [3,4]. The relevant microscopic physical processes driving the dynamical behavior in STNOs are of significant fundamental interest in this rapidly growing field, in particular, considering their widespread potential for applications in the area of data storage and processing [5]. However, a detailed microscopic understanding of spin-transfer-induced dynamics on the nanoscale is still elusive since it requires a direct quantitative magnetic characterization of the induced excitations at the relevant length and time scales. To address these open questions, we investigated STNOs with perpendicular magnetic anisotropy using scanning transmission x-ray microscopy (STXM) and determined the spatial extent and magnitude of the spin excitations.

We have chosen a STNO with perpendicular magnetic anisotropy because it represents a well-defined model system, where the current direction, remanent field, and magnetic anisotropy field are aligned parallel. This is relevant because the applied field and ferromagnetic layer's magnetic anisotropy are predicted to determine the nature of the excited spin-wave modes [6–9]. In a magnetic layer with perpendicular magnetic anisotropy that is also magnetized perpendicularly to the film plane, spin waves

excited by an electrical current have a frequency that is less than the lowest propagating spin-wave mode, which coincides approximately with the ferromagnetic resonance frequency and are, therefore, expected to be strictly localized in the contact region. It has been predicted and inferred indirectly from electrical measurements that these localized excitations are dissipative solitons—localized excitations that balance exchange and magnetic anisotropy forces [8,10,11].

Here we report the direct observation of current-induced magnetic solitons using synchrotron-based scanning transmission x-ray microscopy. X-ray magnetic circular dichroism (XMCD) is employed to detect changes in the average direction of the magnetization. XMCD is a common method to study magnetic properties in an element-specific manner [12,13]. It directly probes the spin polarization of the valence electronic states via x-ray-induced excitation of core-level electrons. Small changes of the magnetization of 10^{-4} or less can be recorded with a spatial resolution of about 35 nm using state-of-the-art x-ray optics in combination with a synchrotron as a tunable, polarized, and pulsed soft x-ray source [14,15].

Finally, due to the ability of x-rays to penetrate a few micrometers of material, we are able to study isolated buried magnetic layers. Altogether, these capabilities enable us to observe spin excitations in the magnetic region right *beneath* the nanocontact where the current is injected and in its direct vicinity. In our samples where the free magnetic layer exhibits perpendicular anisotropy, we used this approach to observe changes in magnetization as a function of the current. Our STXM images reveal an abrupt onset of a magnetic soliton excitation at a threshold current that is localized in the contact area. However, the amplitude

of the excitation is far less than that predicted [8], showing that the spin dynamics is not described by existing models.

Our STNOs consist of Cu nanocontacts (150 nm in nominal diameter) to a CoNi multilayer with perpendicular anisotropy and an in-plane magnetized fixed layer (permalloy), the same layer stack as those studied in Ref. [11]. The CoNi multilayer (0.2 nm Co|0.6 nm Ni) \times 6|0.2 nm Co and permalloy are separated by 10 nm of Cu, which is sufficiently thick to completely decouple the layers magnetically. The layer stack was grown on 100 nm thick SiN membranes that are required as a transparent substrate for the soft x-ray transmission experiments. The membrane was coated with a 500 nm thick Al layer on the back side to increase the thermal conductivity. Since the microscopy experiments were conducted in a vacuum environment, the Al layer was crucial for the thermal stability of the device, as we will show later.

We first characterized our samples *ex situ* using ferromagnetic resonance spectroscopy, both directly after layer deposition and after STNO and membrane fabrication. The effective anisotropy field of the CoNi free layer was $\mu_0 H_{\text{eff}} = \mu_0(H_K - M_s) = 0.25$ T [16], with $\mu_0 H_K = 0.99$ T and $\mu_0 M_s = 0.74$ T, indicating a strong perpendicular magnetic anisotropy. Measurements before and after fabrication showed no change in the material properties. To further determine the current needed to excite magnetization dynamics, we carried out electrical transport measurements. The electrical resistance between two magnetic layers across a nonmagnetic layer depends on the relative orientation of their magnetizations due to the giant magnetoresistance effect. The onset of a magnetic excitation can, therefore, be detected by the presence of a peak in the differential dV/dI [11], since the average magnitude of a component of the magnetization changes. We then repeated the measurements in vacuum to corroborate that the Al layer serves as an effective thermal sink to counteract the reduced thermal conductivity in vacuum as designed. For this purpose, the sample was mounted in the same configuration as used in the microscopy experiments. The two curves are shown in Fig. 1(a). A pronounced peak appeared at a current of 29 mA, and no significant differences were observed between *in situ* and *ex situ* measurements.

To image the spin excitations, we then used the STXM instrument at beam line 13-1 at the Stanford Synchrotron Radiation Lightsource [15,17]. The incident photon energy was tuned to the Co L_3 edge (778.1 eV) to make use of the element specificity and only probe changes in the magnetization in the free layer, which is the only layer in the STNO that contains Co. The x-ray beam was aligned perpendicularly to the sample surface, as illustrated in Fig. 1(b), and a static magnetic field of 0.7 T was applied perpendicularly to the sample plane using a permanent magnet. As the absorption is proportional to the dot product of the magnetization \mathbf{M} and the helicity \mathbf{P} of the circularly polarized light [12], the change of the perpendicular

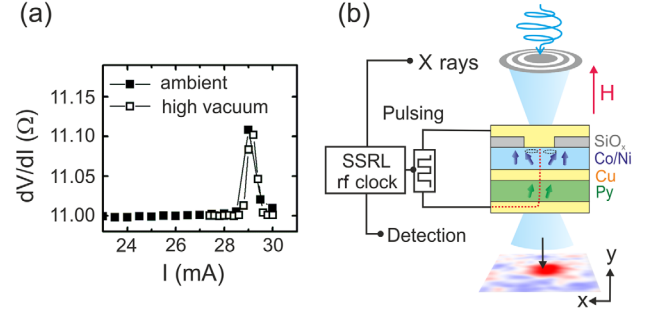


FIG. 1 (color online). (a) STNO electrical characteristics: differential resistance dV/dI versus current I in a perpendicular applied field of 0.7 T. The peak at 29 mA marks the threshold for current-induced excitations. It occurs at the same current both in ambient conditions (filled squares) and high vacuum (open squares). (b) Schematic of the STXM instrument and the STNO sample. A Fresnel zone plate was used to focus the x-ray beam to a 35 nm spot, which was scanned across the area around the nanocontact, indicated as the yellow region contacting the Co|Ni layer through the SiO₂ dielectric, to acquire an image. The x-ray detection was synchronized with the x-ray pulses from the synchrotron (rf clock) at 476.2 MHz.

component of magnetization (M_z) can be determined in this geometry. The transmitted x-ray pulses were detected and amplified via an avalanche photodiode and registered using a software-defined photon-counting system [18] that effectively acts as a lock-in amplifier operating at the x-ray pulse repetition rate of the synchrotron at 476.2 MHz. In addition, we modulated the applied current at 640 kHz synchronized with the frequency corresponding to the completion of one full electron orbit in the storage ring. We then compared the transmitted x-ray intensity for the current on and off cycles, i.e., excitation on and off, for each image point. This double lock-in scheme allowed us to detect tiny changes in the x-ray transmission ($\approx 4 \times 10^{-4}$) induced by the current by eliminating long-term drifts and provided a reliable normalization scheme.

Before we discuss the observed excitations, we establish the effective magnetic thickness of the material by measuring the static XMCD effect of the Co layers. This will be important to evaluate the dynamic changes in magnetization in a quantitative manner. We compared the transmission for positive (“+”) and negative x-ray helicities (“−”) corresponding to parallel and antiparallel alignment between the magnetization and the polarization (i.e., \mathbf{M} and \mathbf{P}). The ratio of the intensities is given by

$$\ln(I_+^*/I_-^*) = (\mu_+ - \mu_-)t = \Delta\mu t, \quad (1)$$

where $I_{\pm}^* = I_{\pm}/I_{0,\pm}$ is the normalized beam intensity after transmission through the sample, $I_{0,\pm}$ the beam intensity, μ_{\pm} the spin-dependent absorption coefficient, and t the layer thickness. We obtained an XMCD contrast that corresponds to a Co thickness of ~ 1.3 nm, very close to the nominal Co thickness in the free layer of 1.4 nm.

We then recorded STXM images as a function of the applied current. Figures 2(a) and 2(b) show XMCD images with the nanocontact region outlined with a dashed line. For currents less than 29 mA, we did not observe any XMCD contrast in our STXM images [see Fig. 2(a)]. However, at a current of 29.9 mA, we detected a pronounced excitation around the position of the nanocontact. This suggests that the observed feature appears abruptly at a current between 28.8 and 29.9 mA. The fact that the observed contrast reverses its sign upon reversing the polarization is the signature of an XMCD effect caused by a change in M_z . Figure 2(b) shows images at three different applied current values above the threshold current for both x-ray helicities, whereas the + helicity shows an increase in the x-ray transmission (a red signal) and the - helicity shows a decrease (a blue signal) in the x-ray transmission. This observation is consistent with a decrease of the average value of M_z . We observed magnetic dichroism in all images obtained with currents between 29.9 and 34.3 mA, the largest current we applied. Although the spatial extension of the observed excitations is mostly symmetric, some cases exhibit an elliptical deformation. We do not believe this represents a change in the vertical

extent of the excitation. Considering that it takes 60 to 90 minutes to acquire a single image, we attribute this deformation to small vertical drifts of the incident x-ray beam that cannot be compensated and lead to small changes in the vertical scale [19].

We continue by quantitatively analyzing the image contrast by constructing one-dimensional profiles through the area of the nanocontact. This is shown in Fig. 3(a) for a current of 31.0 mA in an image acquired with a negative x-ray helicity. Each point (black squares) represents an average of the raw (unfiltered) XMCD data over a half-circle at a certain distance to the right (+ x) and left (- x) of the center of the nanocontact. We observe that the absorption signal decays rapidly outside of the nanocontact, having a full width at half maximum of ≈ 175 nm, just slightly larger than the nominal diameter of the contact (150 nm). It is instructive to compare the measured spin-wave excitation profiles to theoretical predictions. First, we consider a propagating mode predicted by Slonczewski in a model that describes small amplitude excitations by linearizing the Landau-Lifschitz-Gilbert-Slonczewski (LLGS) torque equation [20]. This is shown as a dashed line in Fig. 3(a). The envelope of the propagating mode clearly fails to describe the measured excitations, as it predicts a

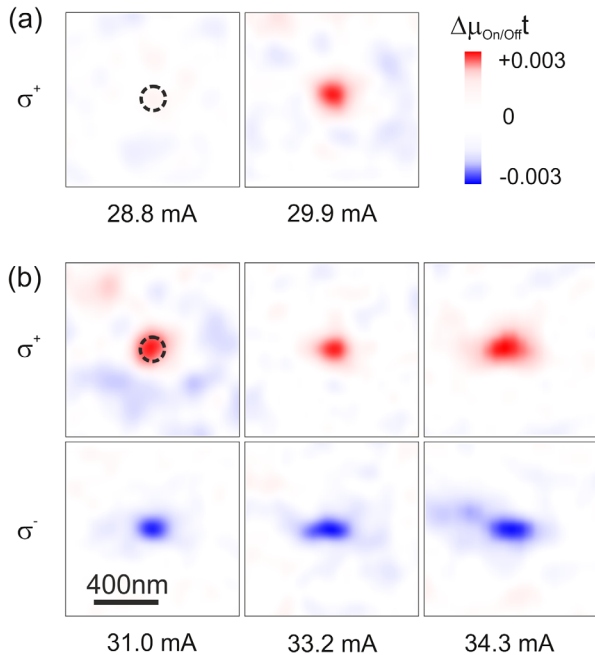


FIG. 2 (color online). XMCD images of the nanocontact region at applied currents of (a) 28.8 and 29.9 mA taken with positive helicity and (b) 31.0, 33.2, and 34.3 mA taken with both positive and negative x-ray helicities. The nanocontact is located in the center of each image, indicated with dashed circles in some of the images. The positive contrast in the nanocontact region for positive helicity and negative contrast for negative helicity is consistent with a reduced magnetization component (M_z) in the contact region above the threshold current. The images shown have 21 by 21 pixels and have been smoothed with a Gaussian filter with a standard deviation of 1 pixel or 50 nm.

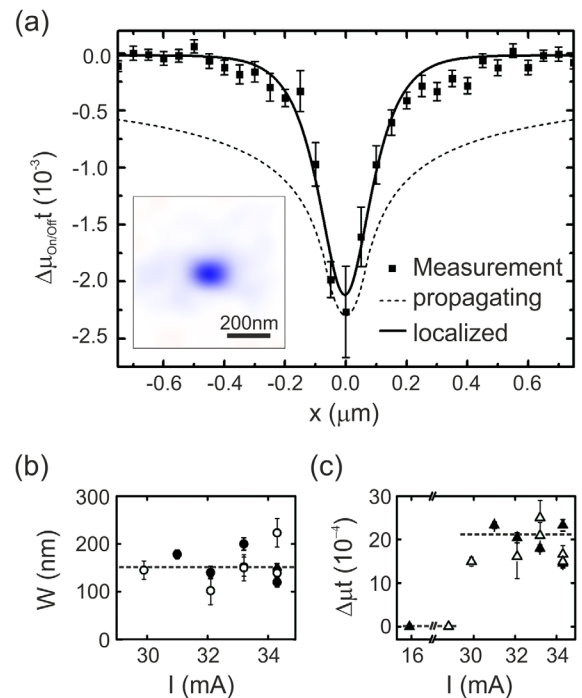


FIG. 3 (color online). (a) Dynamic XMCD contrast (black squares) as a function of the distance x from the nanocontact center for a current of +31.0 mA at negative x-ray helicity. The measurement is compared to a linear propagating mode (dashed line) and to a localized mode (solid line). (b) Width of the localized modes (disks) and (c) amplitude (triangles) at different currents for negative (filled symbols) and positive (open symbols) x-ray helicity.

longer decay length and a larger excitation amplitude outside the contact region. Also, the Slonczewski mode has only small amplitude excitations in the contact, and our data show that the excitations have a large amplitude. Proposed corrections to the propagating modes that account for the nonlinearities [21] show a similar (i.e., slow) decay and, thus, also do not fit our data.

Second, we plot the expected form of a soliton mode [22], a nonlinear, symmetric, and localized mode [see the line in Fig. 3(a)]. This localized mode profile is a good fit to our data. We used a hyperbolic secant as the profile for the soliton mode derived from the LLGS equation for a perpendicularly magnetized film [22]. The profile of this soliton mode is a good approximation to localized modes described as bullet modes for in-plane magnetized layers [6] and droplet soliton modes for layers with perpendicular magnetic anisotropy [8]. We can also extract the mode amplitude that corresponds to the magnitude of the absorption at the contact center and the mode width that characterizes the size of the localized excitation from raw (unfiltered) STXM data. This is shown in Figs. 3(b) and 3(c) as a function of the applied current. The mode width fluctuates (≈ 175 nm) with no particular trend as a function of the applied current. We believe that these variations are likely due to sample stage drift and our image processing: we measured images at the same currents more than once and obtained slightly different values, as shown in Fig. 3(b). The onset of excitations occurs between 29 and 30 mA in the current increment we have chosen to acquire the data shown in Fig. 3(c). By comparing the maximum amplitude of the excitations [see Fig. 3(c)] to the absolute XMCD contrast (i.e., the contrast representing a 180° change of the magnetization), the precession cone angle $\theta_p(r)$ can be determined from $\theta_p = \arccos(1 - \Delta\mu_{\text{on/off}}(r)/\Delta\mu_{+/-})$. Thus, the amplitude of the peak in absorption indicates precession angles of about $25^\circ \pm 2.1^\circ$ at the center of the soliton.

Several conclusions can be drawn from the analysis of the x-ray images. First, the observed excitation is localized at the nanocontact and exhibits almost circular symmetry. Second, its abrupt onset and large amplitude indicates that it is formed due to a nonlinear response of the magnetization to the applied spin-transfer torque. Third, the amplitude profile is consistent with that of a magnetic soliton as described by Kosevich *et al.* [22], but its overall amplitude clearly indicates that the magnetic moments in the soliton are not completely reversed, as was predicted by theory. The theory of dissipative droplet solitons predicts an abrupt onset of spin excitations at a threshold current and a large amplitude response, which describes our experimental findings well [8]. However, the theory also predicts a nearly complete reversal of the magnetization near the center of the contact that we have not observed.

There are several possible reasons for the discrepancy between the theory and experiment. First, the theory does

not consider the effect of thermal fluctuations on the magnetization dynamics. Our previous magnetoresistance measurements using the same type of samples at low temperature (4.2 K) and in the same range of applied fields (≈ 0.7 T) indicate a nearly complete magnetization reversal in the contact region [11]. However, our measurements as a function of temperature up to and above room temperature show a decreased response (step in contact I - V characteristics and magnetoresistance) with increasing temperature [23]. This is strong evidence that thermal fluctuations play an important role in the dynamics. Second, another factor that is not considered in the theory is disorder; in the theory, the materials are assumed homogeneous. However, the devices are composed of polycrystalline films with disorder, including spatial variations in the magnetic anisotropy and magnetization. Third, the theory does not consider Oersted fields associated with the current. Finally, the droplet may move or have internal dynamics in response to thermal fluctuations or other forces that could lead to a smaller time-averaged precession angle at the contact center; e.g., the droplet may diffuse or orbit around the contact or it may periodically annihilate and renucleate. The integration time in our STXM experiments is 500 ms per point in the image and would, thus, not resolve such droplet dynamics which likely occurs on shorter time scales.

In summary, we have directly observed a spin-transfer-torque excited magnetic soliton in a nanocontact to a CoNi multilayer with perpendicular magnetic anisotropy having an equivalent Co thickness of only 1.4 nm. Spatial images provide a precise measurement of the soliton profile and amplitude: we have determined the soliton full width at half maximum to be ~ 175 nm, similar to the nominal diameter of the nanocontact (150 nm), and a maximum angle precession of $\sim 25^\circ$. Our results also have demonstrated the potential of STXM to resolve spin wave excitations at nanometer length scales in specific magnetic layers in complex layer structures within nanostructured devices and provided a test of basic models along with a deeper understanding of the nature of current-induced magnetic excitations.

We thank Mark Hoefer for his discussions of and comments on this manuscript. F. M. acknowledges support from the European Commission (Grant No. MC-IOF 253214), from Catalan Government COFUND-FP7, and from the Spanish Government (Grant No. MAT2011-23698.) S. B. gratefully acknowledges support from the Knut and Alice Wallenberg Foundation. This research was supported by NSF-DMR-1309202 and in part by U.S. Army Research Office ARO-MURI Grant No. W911NF-08-1-0317. STNOs were fabricated at the Center for Functional Nanomaterials, Brookhaven National Laboratory, which is supported by the U.S. Department of Energy, Office of Basic Energy Sciences under Contract No. DE-AC02-98CH10886. Experiments at the Stanford

Synchrotron Radiation Light Source, SLAC National Accelerator Laboratory are supported by the U.S. Department of Energy, Office of Basic Energy Sciences under Contract No. DE-AC02-76SF00515.

*dirk.backes@web.de

- [1] W. H. Rippard, M. R. Pufall, S. Kaka, S. E. Russek, and T. J. Silva, Direct-Current Induced Dynamics in $\text{Co}_{90}\text{Fe}_{10}/\text{Ni}_{80}\text{Fe}_{20}$ Point Contacts, *Phys. Rev. Lett.* **92**, 027201 (2004).
- [2] T. J. Silva and W. H. Rippard, Developments in nano-oscillators based upon spin-transfer point-contact devices, *J. Magn. Magn. Mater.* **320**, 1260 (2008).
- [3] V. E. Demidov, S. Urazhdin, and S. O. Demokritov, Direct observation and mapping of spin waves emitted by spin-torque nano-oscillators, *Nat. Mater.* **9**, 984 (2010).
- [4] M. Madami, S. Bonetti, G. Consolo, S. Tacchi, G. Carlotti, G. Gubbiotti, F. B. Mancoff, M. A. Yar, and J. Åkerman, Direct observation of a propagating spin wave induced by spin-transfer torque, *Nat. Nanotechnol.* **6**, 635 (2011).
- [5] F. Macià, A. D. Kent, and F. C. Hoppensteadt, Spin-wave interference patterns created by spin-torque nano-oscillators for memory and computation, *Nanotechnology* **22**, 095301 (2011).
- [6] A. Slavin and V. Tiberkevich, Spin Wave Mode Excited by Spin-Polarized Current in a Magnetic Nanocontact is a Standing Self-Localized Wave Bullet, *Phys. Rev. Lett.* **95**, 237201 (2005).
- [7] M. A. Hoefer, T. J. Silva, and M. D. Stiles, Model for a collimated spin-wave beam generated by a single-layer spin torque nanocontact, *Phys. Rev. B* **77**, 144401 (2008).
- [8] M. A. Hoefer, T. J. Silva, and M. W. Keller, Theory for a dissipative droplet soliton excited by a spin torque nanocontact, *Phys. Rev. B* **82**, 054432 (2010).
- [9] S. Bonetti, V. Tiberkevich, G. Consolo, G. Finocchio, P. Muduli, F. B. Mancoff, A. Slavin, and J. Åkerman, Experimental Evidence of Self-Localized and Propagating Spin Wave Modes in Obliquely Magnetized Current-Driven Nanocontacts, *Phys. Rev. Lett.* **105**, 217204 (2010).
- [10] S. M. Mohseni, S. R. Sani, J. Persson, T. N. A. Nguyen, S. Chung, Y. Pogoryelov, P. K. Muduli, E. Iacocca, A. Eklund, R. K. Dumas, S. Bonetti, A. Deac, M. A. Hoefer, and J. Åkerman, Spin Torque-Generated Magnetic Droplet Solitons, *Science* **339**, 1295 (2013).
- [11] F. Macià, D. Backes, and A. D. Kent, Stable magnetic droplet solitons in spin-transfer nanocontacts, *Nat. Nanotechnol.* **9**, 992 (2014).
- [12] B. T. Thole, P. Carra, F. Sette, and G. van der Laan, X-ray Circular Dichroism as a Probe of Orbital Magnetization, *Phys. Rev. Lett.* **68**, 1943 (1992).
- [13] C. T. Chen, Y. U. Idzerda, H.-J. Lin, N. V. Smith, G. Meigs, E. Chaban, G. H. Ho, E. Pellegrin, and F. Sette, Experimental Confirmation of the X-Ray Magnetic Circular Dichroism Sum Rules for Iron and Cobalt, *Phys. Rev. Lett.* **75**, 152 (1995).
- [14] P. Fischer and H. Ohldag, X-rays and Magnetism, *Rep. Prog. Phys.* **78**, 094501 (2015).
- [15] S. Bonetti, R. Kukreja, Z. Chen, D. Spoddig, K. Ollefs, C. Schöppner, R. Meckenstock, A. Ney, J. Pinto, R. Houanche, J. Frisch, J. Stöhr, H. Dürr, and H. Ohldag, Microwave soft x-ray microscopy for nanoscale magnetization dynamics in the 5–10 GHz frequency range, [arXiv:1504.07561](https://arxiv.org/abs/1504.07561).
- [16] F. Macià, P. Warnicke, D. Bedau, M.-Y. Im, P. Fischer, D. A. Arena, and A. D. Kent, Perpendicular magnetic anisotropy in ultrathin CoNiCo/Ni multilayer films studied with ferromagnetic resonance and magnetic x-ray microspectroscopy, *J. Magn. Magn. Mater.* **324**, 3629 (2012).
- [17] S. Bonetti, R. Kukreja, Z. Chen, F. Macià, J. M. Hernández, A. Eklund, D. Backes, J. Frisch, J. A. Katine, G. Malm, A. D. Kent, S. Urazhdin, J. Stöhr, H. Ohldag, and H. Dürr, Direct observation and imaging of a spin-wave soliton with p-like symmetry, [arXiv:1504.00144](https://arxiv.org/abs/1504.00144).
- [18] Y. Acremann, V. Chembrolu, J. P. Strachan, T. Tylliszczak, and J. Stöhr, Software defined photon counting system for time resolved x-ray experiments, *Rev. Sci. Instrum.* **78**, 014702 (2007).
- [19] We note that we observed a much smaller and less localized signal at negative applied currents, even for currents less than 29 mA. However, the electrical measurements do not indicate that a negative current induces any magnetization dynamics. The x-ray data obtained with negative current are challenging to quantify because of the weakness of the signal. We speculate that heating of the point contact due to the current could result in additional variations of the magnetization in the free layer, but due to the weakness of the signal, it does not affect the interpretation of the data obtained with positive current.
- [20] J. C. Slonczewski, Excitation of spin waves by an electric current, *J. Magn. Magn. Mater.* **195**, L261 (1999).
- [21] M. A. Hoefer, M. J. Ablowitz, B. Ilan, M. R. Pufall, and T. J. Silva, Theory of Magnetodynamics Induced by Spin Torque in Perpendicularly Magnetized Thin Films, *Phys. Rev. Lett.* **95**, 267206 (2005).
- [22] A. M. Kosevich, B. A. Ivanov, and A. S. Kovalev, Magnetic Solitons, *Phys. Rep.* **194**, 117 (1990).
- [23] S. Lendínez, N. Statuto, D. Backes, A. D. Kent, and F. Macià, Observation of droplet soliton drift resonances in a spin-transfer-torque nanocontact to a ferromagnetic thin film, [arXiv:1507.08218](https://arxiv.org/abs/1507.08218).